Molecular Crystals and Liquid Crystals
Publication details, including instructions for authors and subscription information:
http://www.tandfonline.com/loi/gmcl16

Heat Pulse Propagation in Anthracene Crystals

V. L. Broude

Version of record first published: 14 Oct 2011.

To cite this article: V. L. Broude (1980): Heat Pulse Propagation in Anthracene Crystals, Molecular Crystals and Liquid Crystals, 57:1, 9-21

To link to this article: http://dx.doi.org/10.1080/00268948008069815

Mol. Cryst. Liq. Cryst., 1980, Vol. 57, pp. 9–22
0026-8941/80/5701-0009$04.50/0

Printed in U.S.A.

Heat Pulse Propagation in Anthracene Crystals

V. L. BROUDE

The present paper is the result of our efforts[1,2] to experimentally detect the condensation of excitons into a dielectric liquid. We believe that such a liquid should have a short life-time and therefore its study should involve time-resolved spectroscopic techniques.

Figure 1 schematically shows the experimental setup which permitted us to measure time-resolved fluorescence spectra. Fluorescence recording was

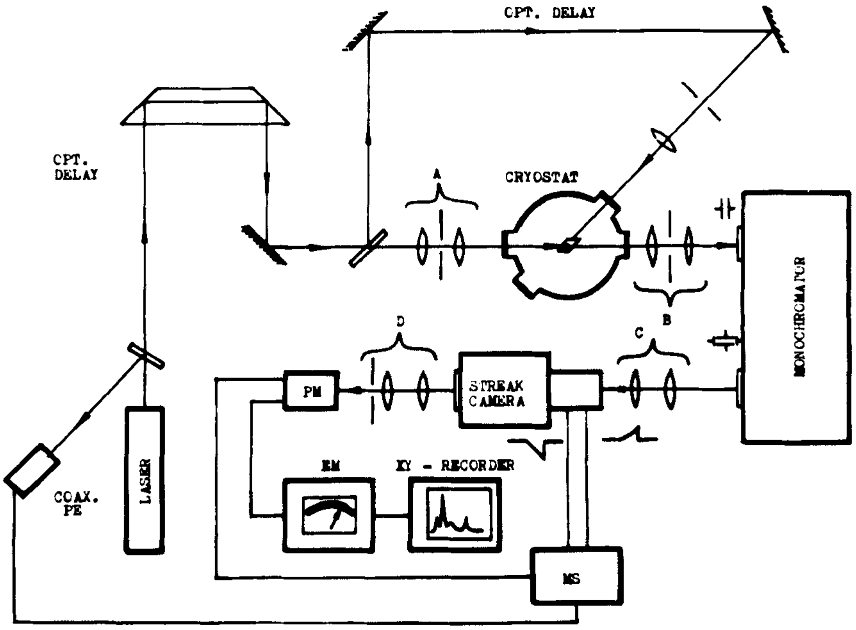

FIGURE 1 Schematic diagram of the experimental setup used for spectral-temporal study of fast non-equilibrium processes[1]. A, B, C, D are optical systems for the formation of the exciting spot on the crystal surface and luminescence detection.

performed in a stroboscopic regime with the aid of a four-stage image converter with a saw-tooth sweep voltage. Information was read from the screen of the image converter and we could obtain either a time-swept signal for a fixed wave-length or a spectrum at a given moment of time (both with the pump pulse on or after it) using the attenuated probe pulse. With this technique we have succeeded to observe short temporal variations in the anthracene crystal fluorescence spectrum at low temperatures under high optical pumping.

For a while we supposed that these spectral-temporal variations unambiguously demonstrated that an exciton condensate was formed in the crystal. However it was tacitly implied that the sample was homogeneously heated throughout its depth during the pump pulse. In fact such an assumption was not fully correct because the propagation and successive reflections of various non-equilibrium phonon groups from both surfaces of the thin single-crystalline plate were not taken into account and so the effective

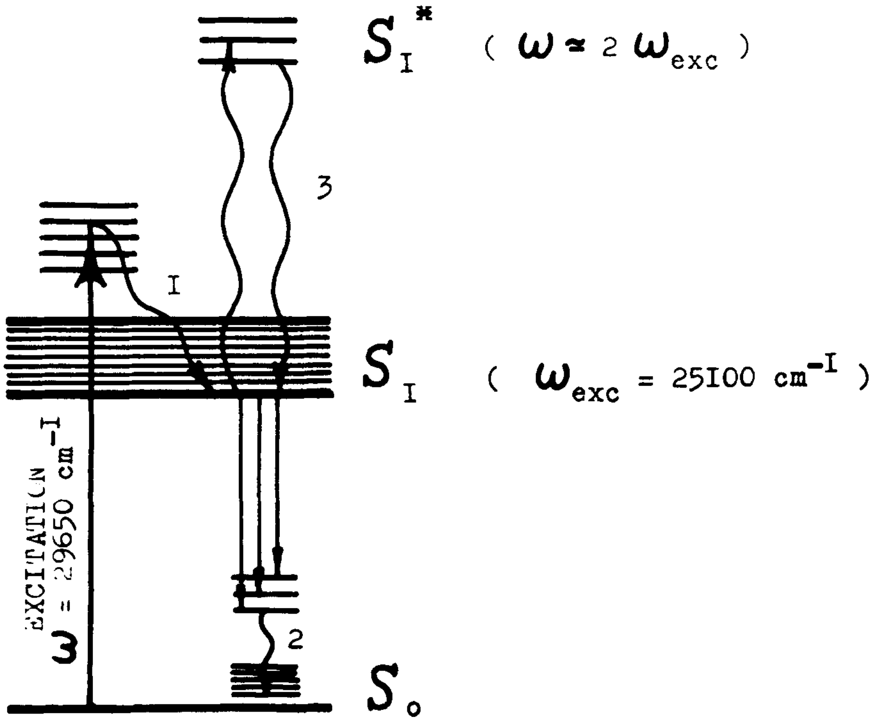

FIGURE 2 Relaxation processes in the anthracene crystals under high intensity optical pumping.

temperature in different points of the sample was not uniform. Therefore our new study of non-equilibrium phonons propagation processes should enable us to make necessary corrections in the results of exciton condensation experiments.

The generation of non-equilibrium acoustic phonons in the crystal with intensive optical pumping results from the following processes:

1) Relaxation of light-generated electron excitation down to the lowest exciton zone.

2) Depopulation of high-frequency phonon crystal states corresponding to intra-molecular vibrations and populated by luminescent vibronic transitions.

3) Exciton Auger-recombination (non-linear quenching of fluorescence) when one of the colliding excitons gives its energy to another. The new high electronically excited state relaxes then down to the lowest exciton zone. These relaxation processes in a highly pumped crystal result in the conversion of up to ~95 per cent of incident light energy into the heat, i.e. into phonons.

The light absorption in an anthracene crystal occurs in a relatively thin ($\lesssim 0.5\,\mu$) surface layer. This layer may be considered as a source of acoustic phonons since all the other quasiparticles (excitons, optical phonons) have small ($\lesssim 0.1\,\mu$) diffusion displacement lengths. The non-equilibrium phonons were detected by luminescence spectra excited by the attenuated probe pulse time delayed as compared to the main one. Parameters with pronounced temperature dependance and their dependence on the delay time were recorded, namely: (1) half-width $\Delta\nu$ of phononless vibronic band at $\omega_{\max} = 23692\ \mathrm{cm}^{-1}$ ($0\text{–}0 - 1404\ \mathrm{cm}^{-1}$); (2) intensity ratio R in the triplet band (multiplet) of 0–0 transition phonon side band. $\Delta\nu$ and R values are very sensitive to the exciton (polariton) distribution in the zone and depend on the kinetics of its evolution.

Let us now examine our main experimental results. Figure 3 shows measurement data for a relatively thick crystal ($d \simeq 45\,\mu$) where it was possible to detect three different groups of non-equilibrium phonons arriving at the rear surface of the sample by 15, 23 and 31 ns from the pump pulse start. In these experiments the intensity ratio R for two lines (25036 and 25051 cm^{-1}) in the 0–0 transition phonon side band was measured.

Figure 4 demonstrates the observation of the half-width $\Delta\nu$ oscillations for the vibronic band with $\omega_{\max} = 23692\,\mathrm{cm}^{-1}$ and their dependance on the delay time t_D in a thinner crystal ($L = 12\,\mu$). Oscillations were detected both for the front (1) and the rear (2) surfaces of the crystal. The average values of $\Delta\nu$ near which oscillations occur on both surfaces were found to depend on the pump intensity. These functions are shown in Figure 5. The next figure

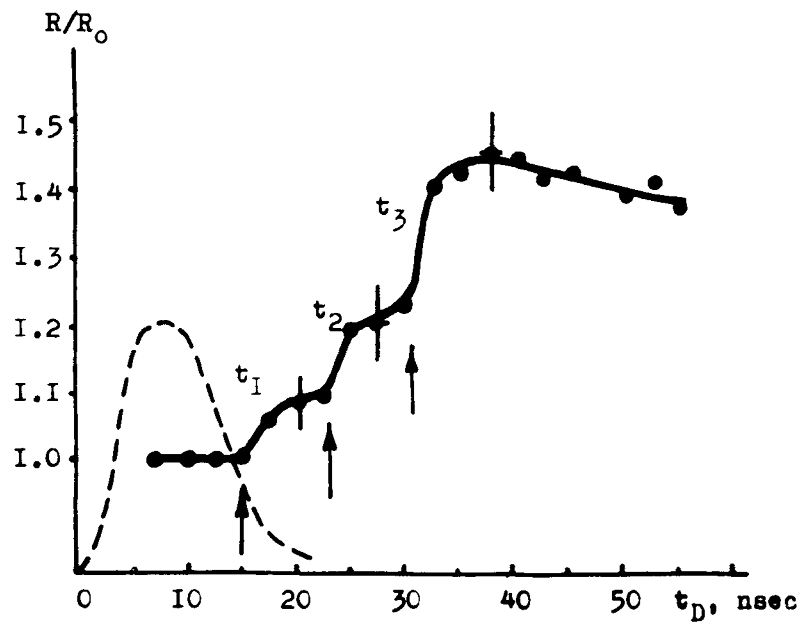

FIGURE 3 Plot of the relative intensity of 25,036 (I) and 25,051 (II) cm^{-1} bands on the rear surface of the 45 μ thick crystal vs, delay time t_D for pump intensity of $P = 40\ \text{kW/cm}^2$ and helium-bath temperature of $T=5\ \text{K}^1$. Arrows mark instants when different phonon groups reach rear surface. R_0 is the intensity ratio for bands I and II for equilibrium regime at $T = 5$ K.

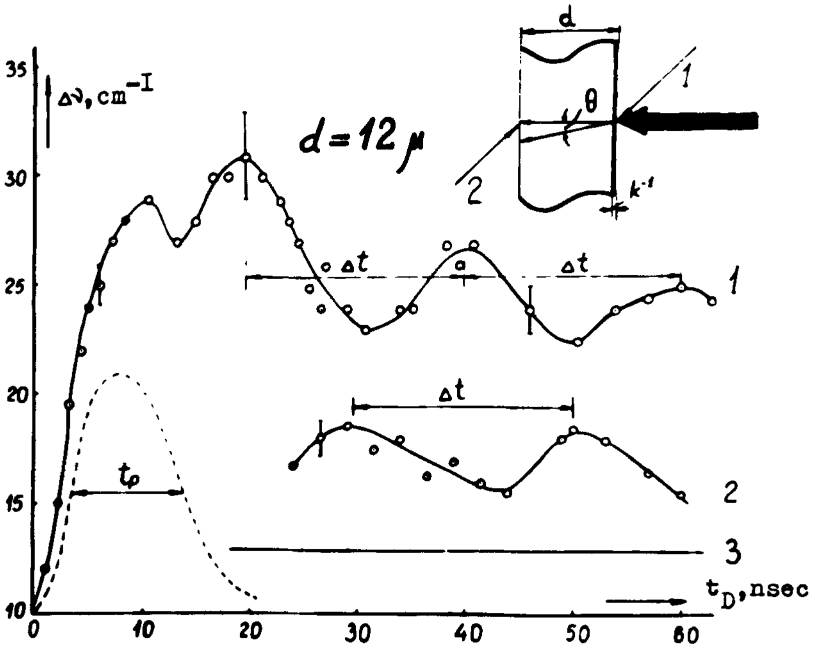

FIGURE 4 Plot of the vibronic (23,692 cm^{-1}) band half-width $\Delta\nu$ on the front (1) and on the rear (2) surfaces vs, delay time for the anthracene crystal 12 μ thick and pump intensity of $P = 40\ \text{kW/cm}^2$ at $T = 5$ K. (3) is the mean value of half-width $\Delta\nu$ on the front and the rear surface for $P = 9\ \text{kW/cm}^2$. Dashed line is the pump pulse shape.

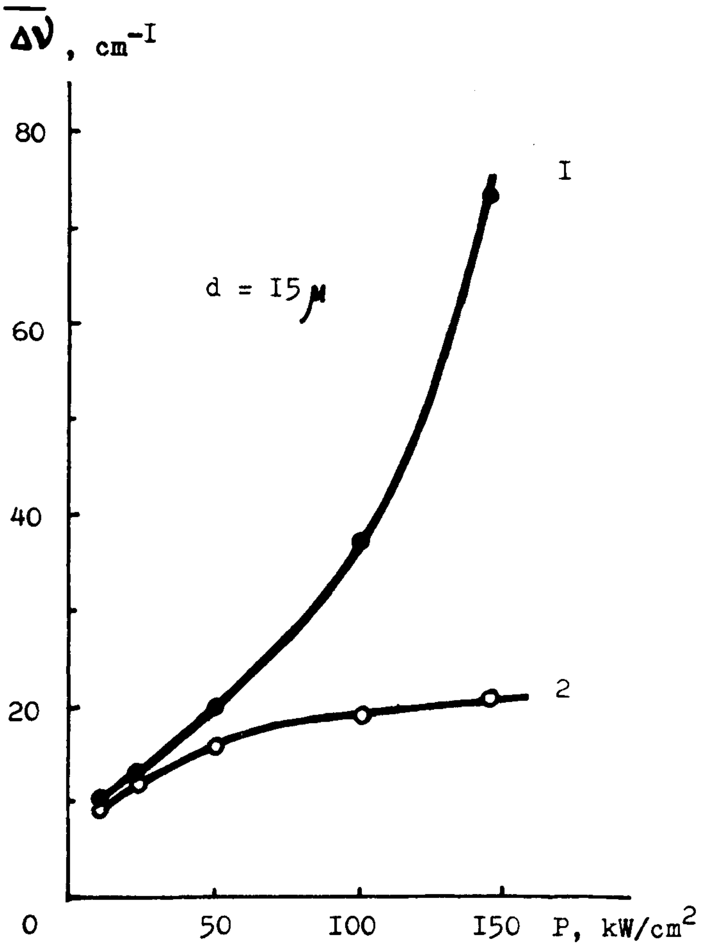

FIGURE 5 Dependence of mean level of half-width $\Delta\nu$ oscillations for the vibronic band 23,692 cm^{-1} on pump intensity for the front (1) and the rear (2) surfaces of anthracene 15 μ thick crystal at $T_0 = 5$ K.

(Figure 6) shows the time dependence of $\Delta\nu$ at the temperature in a thermostat bath of $T_0 = 20$ K. One can see initially rapid and then somewhat slower decrease of the vibronic band (23692 cm^{-1}) half-width $\Delta\nu$ on the front surface and virtually constant small half-width of the band on the rear surface of crystal up to 60 to 70 ns after the pulse start.

What conclusions can be drawn from the experimental results presented here?

1) These experiments suggest the existence of a phonon non-equilibrium in the crystal.

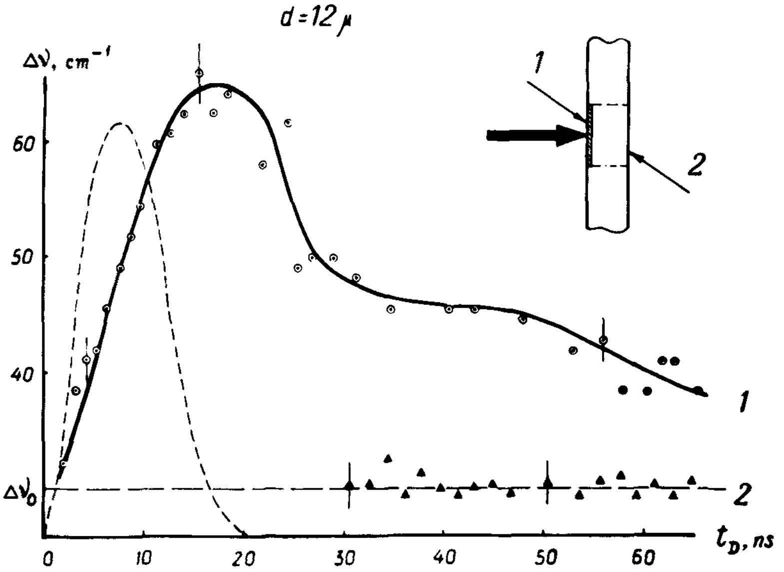

FIGURE 6 Plot of the vibronic 23,692 cm^{-1} band half-width vs. delay time t_D for the front (1) and the rear (2) surfaces and for pump intensity $P = 40$ kW/cm^2. Crystal thickness is 12 μ^1.

2) Propagation time of the non-equilibrium phonon density (i.e. the time a phonon needs to reach rear surface on Figure 3 and the oscillation period on Figure 4) corresponds to the propagation velocity of 1 to 3 × 10^5 cm/s which is close to the speed of sound in this crystal.

3) Difference of the $\Delta\nu$ average levels (and in effect difference of the average temperatures) near which oscillations occur (Figure 4) is a manifestation of the fact that the sample is not heated homogeneously even on an average. As Figure 5 shows the degree of this non-equilibrium grows with pump intensity.

4) Comparison of Figure 4 and Figure 6 suggests that the increase of temperature does not remove phonon density non-equilibrium and non-homogeneity of sample heating but does affect considerably the character of phonon density propagation.

The analysis of these results shows that the observed phonon density propagation may occur only via ballistic or hydrodynamic (or intermediate) regimes. The diffusion propagation (thermoconductivity) being much slower is totally impossible.

To interpret the experimental results a theoretical model of phonon propagation from the front to the rear surfaces of thin single-crystalline plate for different laser pump intensities was developed. The absorption layer

($k^{-1} \lesssim 0.5\,\mu$) is considered as a source of acoustic phonons distributed over the entire Brillouin zone more or less uniformly. High frequency phonons with an energy of about the Debye value $\hbar\omega_D$ make the main contribution to the total energy of the ensemble. To simplify the picture let us assume that the first generation of acoustic phonons created in consequence of internal phonon decay consists of phonons with energy of $\hbar\omega_0$ where $\omega_0 = \omega_D$. Estimates of the phonon occupation number n_0 for these phonons show that $n_0 \ll 1$. This phonon distribution develops initially via spontaneous splitting of one phonon into phonons of lower energy. Simplifying this degradation process we assume that every phonon splits into two phonons of half-the-energy (Figure 7), i.e. that first generation with energy $\hbar\omega_0$ gives second generation with energy $\hbar\omega_0/2$, and then the third generation with $\hbar\omega_0/4$ and so on. As the phonons degrade their life-time increases:

$$\tau(\omega) = \tau_0\left(\frac{\omega_0}{\omega}\right)^5, \qquad \tau_0 \equiv \tau(\omega_0),$$

and consequently the mean free path also rapidly increases $l(\omega) = s\tau(\omega)$ (s is the speed of sound). As long as $n(\omega) \ll 1$ the phonons propagate in the crystal quasiballistically. Typical values of $l_0 = s\tau_0$ are about (10 to 100)a_0 (where a_0 is the lattice parameter), therefore $d \gg l_0$ and this means that rear surface of crystal is reached only by phonons with frequency $\omega \ll \omega_0$. Thus long-wave ballistic phonons propagate in the crystal successively reflecting from both surfaces.

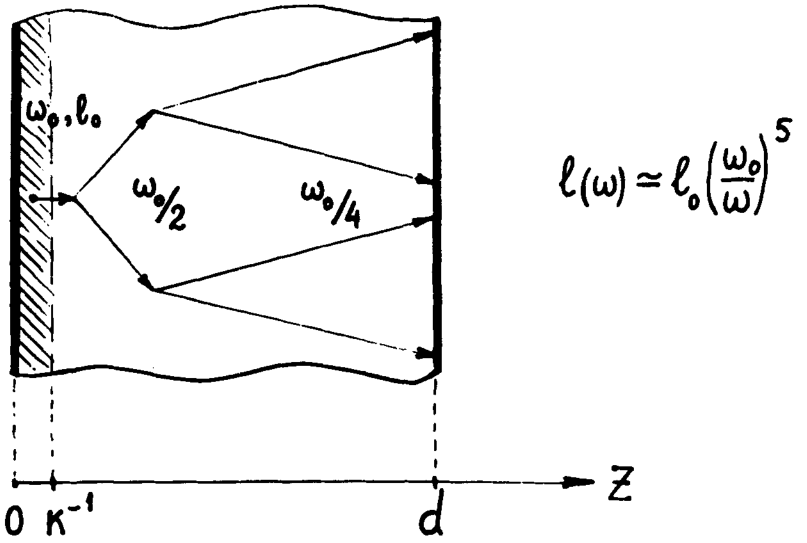

FIGURE 7 Diagram of phonon fission and propagation through the crystal.

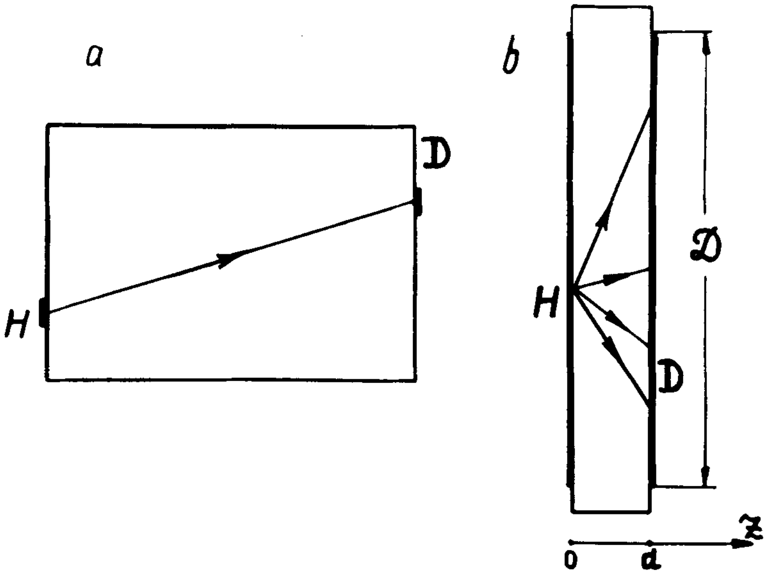

FIGURE 8 Common (a) and flat (b) geometry of experiment. *H* is a heater, *D* is a detector.

It should be emphasized that the existence of temporal oscillations of phonon density in such a quasiballistic system is not obvious. Commonly used geometry of ballistical propagation of thermal pulses implies that phonon generator and detector are much smaller in size than the distance between them. For that reason only phonons propagating in a certain direction and having a certain generator-detector propagation time are detected. In our experiment when transverse size of "generator" and "detector" are large relative to the distance between them phonons propagating in different directions contribute to the signal (Figure 8). Even for an isotropic model of crystal the times of these phonons passing from one surface to another are distributed continuously: $t = d/s \cos\theta$ (where θ is the angle between the propagation direction and the normal to the surface). Therefore a question arises whether an angular averaging would result in a complete vanishing of oscillations? To answer this question the following problem was solved: The phonons are created on the surface of an infinite-area plate according to a given temporal law. The crystal is assumed to be isotropic. The surface emits phonons isotropically as a black body. The generated phonons propagate ballistically to the plate reflecting from its surfaces in either mirror-like or diffusion manner. Numerical calculations for this model demonstrated the existence of well-defined oscillations (Figure 9).

When degradation proceeds the quasiballistical regime considerably changes. The reason is the rapid increase of occupation number for phonon

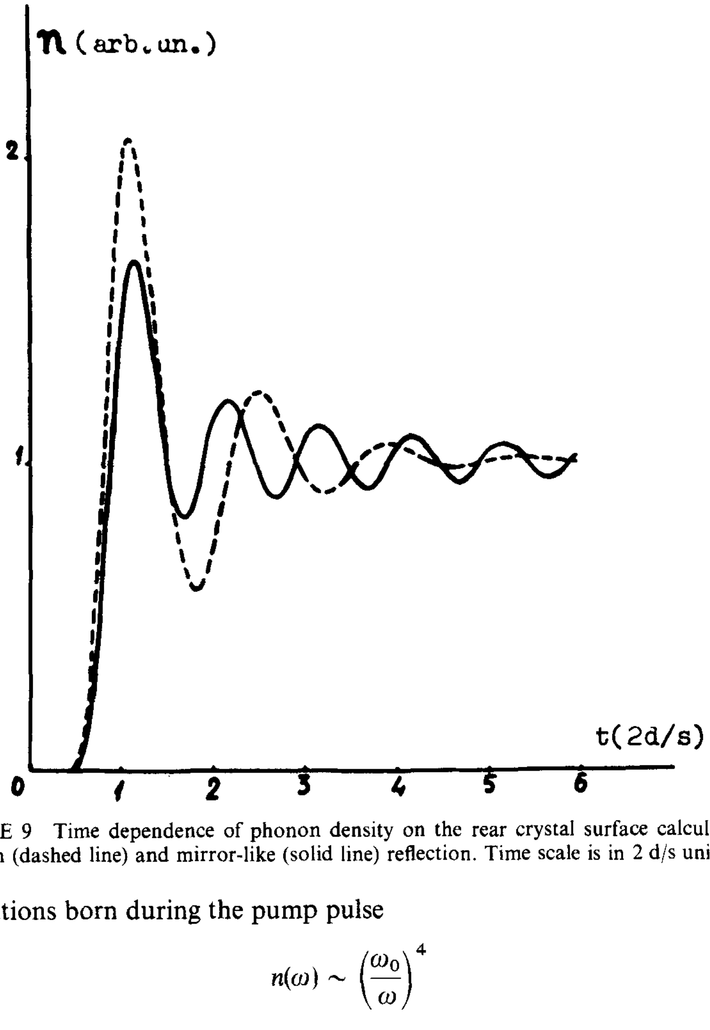

FIGURE 9 Time dependence of phonon density on the rear crystal surface calculated for diffusion (dashed line) and mirror-like (solid line) reflection. Time scale is in 2 d/s units[1].

generations born during the pump pulse

$$n(\omega) \sim \left(\frac{\omega_0}{\omega}\right)^4$$

(this may be easily derived from simple balance equations). For $n(\tilde{\omega}) \simeq 1$ besides spontaneous decay the induced decay and merging processes become significant. These processes thermalize the phonon distribution transforming it into the Planck one with the temperature $\tilde{T} \simeq \hbar\tilde{\omega}$. Thus for $\tilde{\omega} \simeq \omega$ phonon propagation occurs in hydrodynamic or diffusion regime.

To interpret an experiment with a 45 μ-thick crystal (Figure 3) wherein several values of the time the non-equilibrium needs to reach the rear surface were observed, the ballistic phonon propagation was considered with real anisotropy of the anthracene crystal taken into account. The dependence of propagation time $\tau_j(\mathbf{n})$ for the acoustic phonons of the jth branch

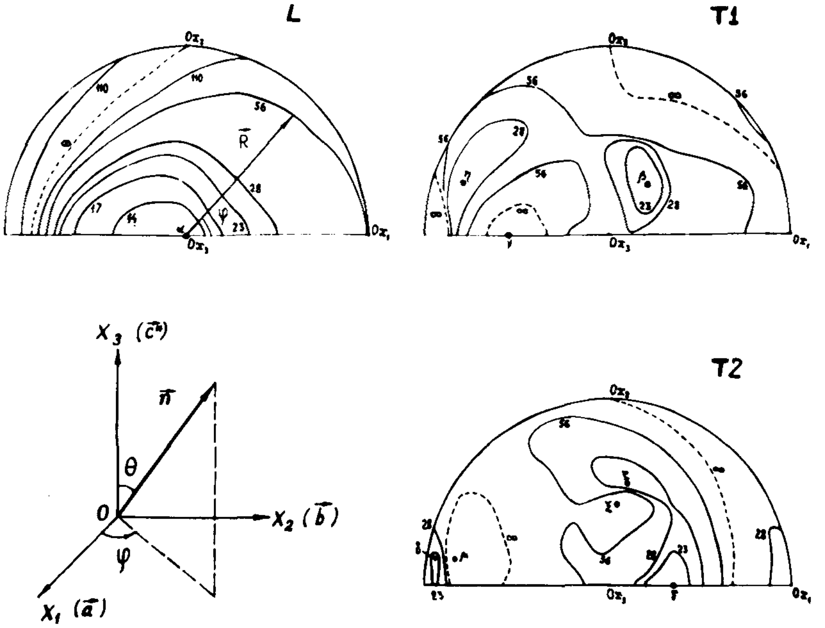

FIGURE 10 Arrival time patterns for quasi-longitudinal (L) and two quasi-transverse (T_1 and T_2) phonon branches[2]. Solid lines connect points with equal arrival time (for the 45 μ thick crystal) marked with numbers at the lines. Heavy points marked with Greek letters correspond to $\tau_j(\mathbf{n})$ function minima. These designations are the same in Table I and on Figure 11. The direction of vector **n** on patterns is given in the polar coordinates. Angle φ between projection of **n** on $0X_1X_2$ plane (ab is crystal plane) and $0X_1$ axis is defined by the angle between this axis and the vector **R** connecting the origin $0X_3$ with any point on the pattern. The angle θ between vector **n** and $0X_3$ axis (normal to ab-plane) is defined by the vector **R** length in the polar diagram equal to $2\sin^2\theta/2$.

(quasilongitudinal L and two quasitransverse T_1 and T_2) on the direction of their wave vector **n** was calculated on the basis of the elastic constants for the anthracene crystal. Figure 10 shows propagation patterns corresponding to all three branches. The phonon density jumps on the rear surface of the crystal were shown to be connected with the function $\tau_j(\mathbf{n})$ minima. The functions minimum values for all three branches for the 45 μ-thick anthracene crystal are summarized in Table I.

The results of calculations are compared with experimental data in Figure 11. One can easily see that calculated values for propagation time ($t_1 = 12.8$, $t_2 = 20.2$, $t_3 = 23$ ns) are in a good agreement with the experimental ones (15 and 23 ns). However the propagation time of 31 ns of the main phonon group seems to correspond to the established hydrodynamic flow in the phonon system.

TABLE I

α	L	12.8
β	T_1	20.2
γ	T_2	20.2
δ	T_2	22.2
ξ	T_2	23.2
η	T_1	23.3
μ	T_2	105
ν	T_1	124

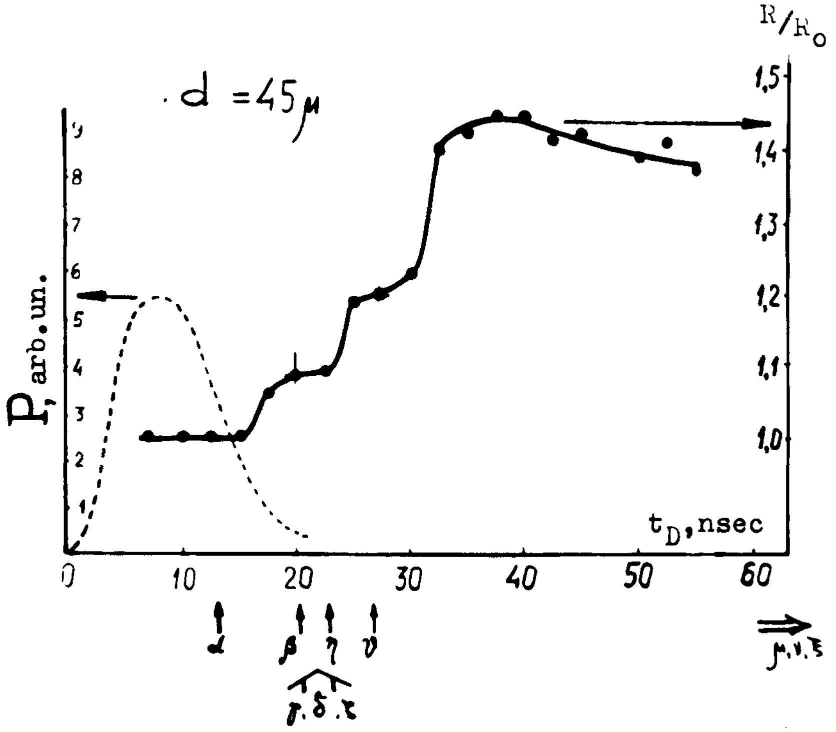

FIGURE 11 Comparison of experimental data[1] on arrival times for various phonon groups with calculated ones[2]. Arrows with Greek letters mark $\tau_j(\mathbf{n})$ function for minima corresponding to phonon density jumps.

Concluding the paper we note that when the sample temperature increases up to $T = 20\,\mathrm{K}$ and pump intensity grows up to $P > 40\,\mathrm{kW/cm^2}$ the observed phenomena are in a good qualitative agreement with the theoretical model taking into account the umklapp processes. As the estimates suggest at $T = 20\,\mathrm{K}$ umklapp processes drastically affect the phonon propagation mode transforming it into a diffusion regime. Similar phenomenon should occur also with the incident light intensity increase.

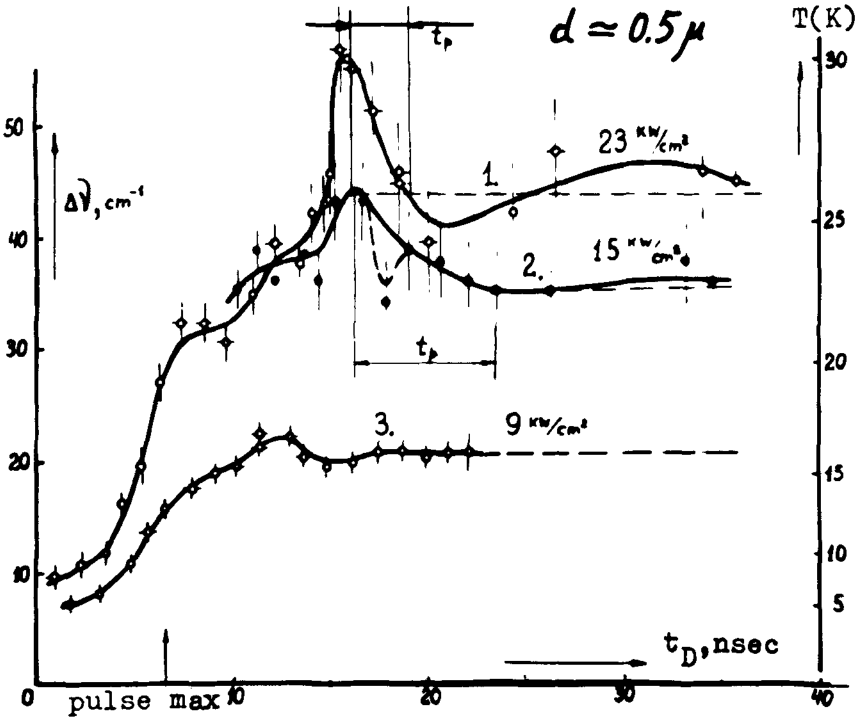

FIGURE 12 Time dependence of 23,692 cm^{-1} band half-width in the 0.5 μ-thick anthracene crystal for various pump intensities and bath temperature of 5 K. Temperature scale corresponds to $\Delta\nu$ and T values in equilibrium conditions.

Returning back to the search for the condensed exciton phase, we understand now from the above that such a phase has to be looked for in thin samples ($d < 1\ \mu$) lacking the conditions for phonon propagation so the phonon density distribution in the sample may be considered uniform.

Figure 12 shows experimental data for a thin sample (thickness d of the order k^{-1}) for different pump intensities. One can see that in this case indeed the sample is rather soon ($t_D \gtrsim 25$ ns) uniformly heated in accordance with the energy pumped into the crystal. Nevertheless the $\Delta\nu$ change was observed at a moment of time near the end of pump pulse and this fact suggests a non-equilibrium in the system. The amplitude of this non-equilibrium and its relaxation rate depend on the pump intensity. If one assumes a non-equilibrium connected with the phonon system, its relaxation time leads to a reasonable estimate for the Debye phonon diffusion path-length of $l_0 \simeq 0.6\ \mu$ which is in a good agreement with the above sequence of different phonon propagation regimes in thick crystals.

However in the framework of this model, the long period of non-equilibrium establishment is still hard to explain. This non-equilibrium might be connected with the exciton condensate. To choose between these alternatives one needs additional experimental data.

Acknowledgment

The contents of this paper were presented in talks by Broude during his visit to the United States in 1977. This version was prepared by I. I. Tartakovskii and E. F. Sheka and translated by S. V. Broude.

References

1. V. L. Broude, N. A. Vidmont, V. V. Korshunov, I. B. Levinson, A. A. Maksimov, and I. I. Tartakovskii, *Pis'ma JETPh*, **25**, 285, 1977. (*Sov. Physics—JETP Letters*, **25**, 261 (1977)). V. L. Broude, N. A. Vidmont, D. V. Kazakovtzev, V. V. Korshunov, I. B. Levinson, A. A. Maksimov, I. I. Tartakovskii, and V. P. Yashnikov, *JETF*, **74**, 314, 1978. (*Sov. Physics—JETP*, **47**, 161 (1978)).
2. D. V. Kazakovtzev, I. B. Levinson, V. P. Yashnikov, *JETF*, **74**, 328, 1978. (*Sov. Physics—JETP*, **47**, 169 (1978)).